Morphology of Bulk Nylon 6 Subjected to Plane Strain Compression

A. Galeski

Centre of Molecular and Macromolecular Studies, Polish Academy of Sciences, 90-362 Lodz, Poland

A. S. Argon and R. E. Cohen*

Massachusetts Institute of Technology, Cambridge, Massachusetts 02139

Received September 20, 1990; Revised Manuscript Received February 18, 1991

ABSTRACT: The mechanisms of deformation of nylon 6 in plane strain compression were elucidated by density measurements, differential scanning calorimetry, polarized light microscopy, X-ray diffraction, and X-ray diffraction pole figures. A deconvolution procedure for separating overlapping X-ray diffraction peaks and the amorphous halo was used to generate pole figures for the various α- and γ-phase reflections exhibited by nylon 6. At compression ratios above 1.6, specimens experienced intense shear at −45° and +45° with respect to the flow direction. Shear bands were formed most frequently at interspherulitic boundaries. This shearing produced a small volume fraction of γ-phase crystals in samples that originally contained only α crystallinity. The X-ray diffraction studies showed that γ-phase crystals were oriented with their macromolecular chains along the directions of shear bands. The α crystals of nylon 6 underwent extensive deterioration in compression by a chain slip mechanism along the (002) planes containing hydrogen bonds. Slip also caused the rotation of fragmented lamellae that lead, at high compression ratios, to a peculiar bifurcated orientation state resembling a twinned monocrystal.

I. Introduction

It is now well-known that plastic deformation of semicrystalline polymers combines several different mechanisms of deformation of both the crystalline and amorphous phases.[1] Slip along certain crystallographic planes, twinning, martensitic transformations, and lamellar separation have all been reported as common processes in uniaxial straining. The intensity of each mechanism depends on the initial morphology of a sample, the availability of the mechanism in the given crystal structure, the conditions of deformation (i.e., rate, temperature, pressure, etc.), and the size and shape of a sample. Chain slip and kinking have been observed in earlier work[2] on nylon 66 and 610.

Initially spherulitic nylon 6 bulk samples undergo extensive changes during drawing.[3-8] In the equatorial zones of spherulites, where the local radius is nearly perpendicular to the draw direction, the deformation forces the interlamellar material to extend and the radial direction to shorten; lamellae in the 45° fans undergo interlamellar sliding and rotate toward the poles, while polar regions of spherulites are extended along the drawing direction.[8] From the work of Peterlin[9,10] it is known that plastic deformation of semicrystalline polymers destroys and unravels the stacks of thin and long parallel lamellae and transforms them into densely packed microfibrils. Our recent investigations showed that no regular lamellar structure can be distinguished by electron microscopic examination of ultrathin sections of bulk nylon 6 samples that had experienced substantial plastic deformation in uniaxial tension.[8] However, osmium tetroxide (OsO_4) fixation and staining of these deformed samples revealed distinct localized regions of high susceptibility toward OsO_4. These regions were identified as places of locally damaged chemical structure of nylon 6 macromolecules. The location of these regions within the spherulitic structure and the internal substructure of these OsO_4 cross-linked entities indicated that the chemical damage to nylon 6 macromolecules arises from a combination of three sources; mechanical misfit between randomly oriented domains of lamellae within spherulites (see ref 11 for details of nylon 6 domain structure), kinking of lamellae in equatorial zones of spherulites due to shear instability in an amorphous matrix, and shear instability due to chain slip in lamellae in polar zones of spherulites. For samples deformed under uniaxial tension, X-ray diffraction pole figures of deconvoluted peak total intensity show that crystallites of nylon 6 assume orientations with macromolecular chains parallel to the drawing direction.[12] Pole figures of deconvoluted peak widths slow intense disruption of crystals along crystallographic planes containing hydrogen bonds.[12]

In the present paper we present the results of a study of the mechanisms of deformation of bulk nylon 6 samples in plane strain compression in a channel die. As in uniaxial tension, channel die compression also assures uniaxial flow of the polymer; however, the stress field within the sample is quite different from that for uniaxial drawing, and the resulting texture resembles more closely that of a quasi-monocrystal rather than a fiber texture.

II. Experimental Section

Polyamide 6 (Capron 8200 extracted, Allied Corp.) was used in this investigation. A weight-average molecular weight, M_w, of 32 600 g/mol and polydispersity index, M_w/M_n, of 1.80 were determined by size-exclusion chromatography in trifluoroethanol. Plaques of 12-mm thickness, 120-mm length, and 74-mm width were obtained by compression molding. The outer layers of the plaques were removed by machining, and several samples, 74 mm long, 10 mm thick, and of various widths, were cut out from the plaques for further studies. All surfaces of the samples were covered with molybdenum disulfide lubricant for reducing friction in the channel die.

A channel die whose construction is described in detail elsewhere[13] was used for the plane strain compression. Figure 1 shows a sketch of the channel die and defines the three principal directions of deformation, i.e., the compression direction (CD), the free (or flow) direction (FD), and the transverse direction (TD). This channel die is of a similar design to that used by Gray et al.[14] The temperature of the channel die was maintained at 150 °C during the large strain compression flow. The compressive load was applied in steps of 2200-N increments by

0024-9297/91/2224-3953$02.50/0

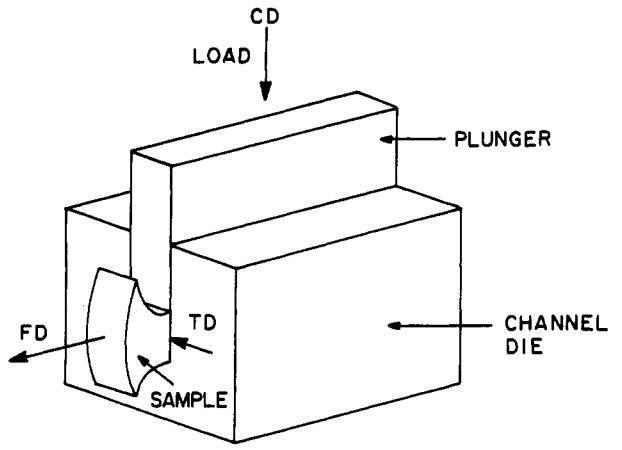

Figure 1. Sketch of channel die, defining the free direction (FD), the compression direction (CD), and the transverse direction (TD).

means of a 100-ton hydraulic press controlled by a minicomputer. After each increment in load, the sample was allowed to deform before the next increment was applied. In order to study the course of deformation and the corresponding changes in morphology, several samples were compressed to different compression ratios. Then the samples were allowed to cool to room temperature in the die, load was released, and the compression ratio was determined from the reduction of the height of the samples. Samples having compression ratios of 1.24, 1.58, 1.84, 2.53, 3.8, and 4.0 were prepared in this manner.

Densities of the samples were determined by means of a density gradient column. The 1-m-high column, covering the range from 1.000 to 1.200 g/cm^3, was filled with a mixture of toluene and carbon tetrachloride. All density measurements were performed at 22 °C. The readout of the positions of the samples in the column was taken 15 min after introducing the samples and after they had come completely to rest.

A Perkin-Elmer DSC IV was used for studying the melting of undeformed nylon 6 specimens. Sample disks of 5-mm diameter and approximately 0.6-mm thickness were cut perpendicular to the free direction of the channel die (the principal direction of extension and molecular alignment). No special attention was given to shrinkage of oriented specimens during DSC runs. The scanning rate was 20 °C/min.

A computerized Rigaku X-ray diffractometer with pole figure attachment was employed in the work. Copper Kα radiation generated at 50 kV and 60 mA from a rotating anode point source was filtered by using electronic filtering and a thin Ni filter. The X-ray diffractometer and the pole figure attachment were controlled on-line by means of a MicroVAX computer running under DMAXB Rigaku-USA software. The applied slit system allowed for collection of the diffracted beam with divergence angles less than 0.3°. Complete pole figures for the projection of Euler angles of sample orientation with respect to the incident beam were obtained; angle α ranged from 0° to 90° in steps of 5°, and angle β varied from 0° to 360° also in 5° steps. It was necessary to connect the X-ray data from transmission and reflection modes to cover the entire pole figure projection plane. The connecting angle was α = 45° for 2θ angles below 33° and α = 30° for 2θ angles above 74°.

The specimens (roughly 2 cm × 2 cm × 1 mm) for X-ray investigations were cut from the oriented samples perpendicular to the free direction. The following diffraction reflections for α and γ crystallographic forms of nylon 6 were of special interest: (200), (002), and (0 14 0) (nearly perpendicular to the molecular axis) for the α phase; (020), (200), and (0 14 0) for the γ phase. The (200) and (002) reflections of the α phase and the (020) and (200) reflections of the γ phase are at 2θ angles in the range from 10° to 30°, while (0 14 0) reflections for both phases are at 2θ angles between 75° to 83°. Due to significant broadening and overlapping of X-ray reflections for nylon 6, the measured diffracted intensity at any 2θ angle is often a superposition of intensities from several peaks and the amorphous halo. Interpretation of the pole figure constructed from such data is not straightforward, and therefore the data were deconvoluted as discussed below.

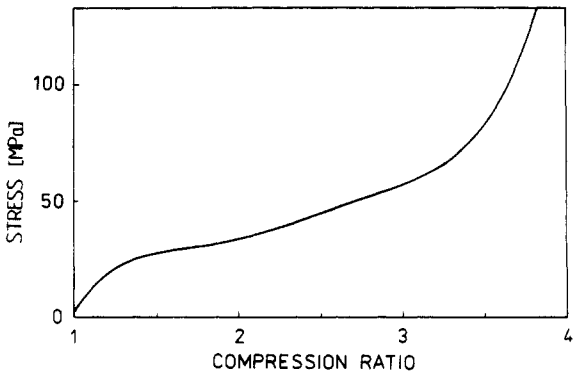

Figure 2. Compressive stress versus compression ratio curve for a 41.3-mm-wide nylon 6 sample compressed in a channel die.

Two sequences of pole figures were collected, the first covering the range of 2θ from 9° to 33° and the second from 74° to 85°, both with steps of $^1/_3$°. For each pair of Euler angles, α and β, an intensity versus 2θ plot was constructed by taking the diffraction intensity value from the pole figure collected at the respective value of 2θ. These diffraction curves were then corrected for absorption and polarization.[15] There were 1387 pairs of Euler angles, hence 1387 diffraction curves for each pole figure of each sample. To each of the diffraction curves the deconvolution procedure, described in detail in a separate paper, was applied.[12] New pole figures were constructed on the basis of total intensities under the deconvoluted peaks for all reflections of interest.

A new type of pole figures based on data for peak width was also constructed for each reflection (for details see ref 12). The newly constructed pole figures must be interpreted as the level contours of the X-ray diffraction peak width of that fraction of crystals that is oriented at Euler angles α and β. The fraction of those crystals is given by the corresponding pole figures of total intensities. X-ray diffraction peaks are sharp only for nearly perfect monocrystals. Polycrystalline samples give broad X-ray reflections, where the lower the number of crystallographic planes producing diffraction in crystallites, the broader is the X-ray diffraction peak.[16] The other sources of widening of X-ray diffraction peaks for polycrystalline samples are residual stresses and local defects, which cause distortions in a regular crystal structure.[16] Considering the above relations the peak width can be treated as a qualitative measure of a mean size of undisturbed crystal structure. The pole figure of peak widths is in fact a map of X-ray averaged sizes of regions with undisturbed crystal structure.

On the basis of deconvoluted X-ray data the degree of crystallinity and the fractions of each crystallographic phase in the samples were determined by integration of intensities in a respective pole figure for each X-ray reflection and the amorphous halo. Morphologies of original compressed samples were also examined by means of a polarizing light microscope. For this purpose 1-μm-thick sections were cut perpendicular to the free direction and parallel to the compression direction with a LKB Ultramicrotome V equipped with glass knives.

III. Results

The nominal compressive stress versus compression ratio curve for a nylon 6 sample (41.3-mm initial height) compressed in a channel die is plotted in Figure 2. It is seen that the initial elastic response of the sample is followed by a region of intense plastic deformation with moderate strain hardening. At a compression ratio of about 2.8, more intense strain hardening begins.

The density change of nylon 6 samples subjected to such plane strain compression in the channel die is presented in Figure 3 as a function of the compression ratio. Initial increase in density is followed by a rapid decrease to a minimum value in the range of compression ratios from

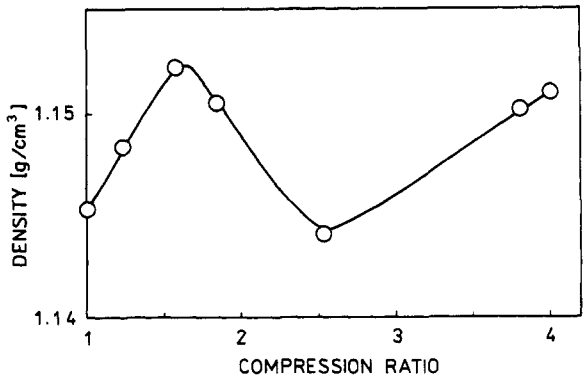

Figure 3. Density change of nylon 6 samples subjected to compression in a channel die.

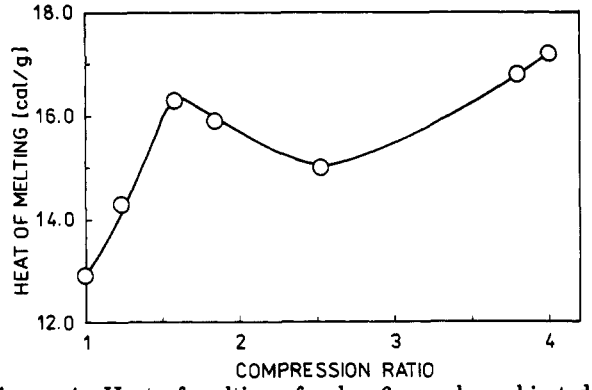

Figure 4. Heat of melting of nylon 6 samples subjected to compression in a channel die.

about 2.5 to 2.6. Further compression results in a new increase of the density of the samples. Comparisons of Figures 2 and 3 suggests that the initial increase in the density is associated with the initial quasi-homogeneous deformation response of the sample under increasing stress while the subsequent decrease in the density can be ascribed to the intense plastic deformation with little accompanying hardening taking place at the compression ratios above 1.5–1.6. For the compression ratios above 2.5–2.6, where more intense strain hardening sets in, the density of the samples increases again though not above the density of samples in the range of compression ratios near 1.5–1.6.

Figure 4 is a plot of the heat of melting of the plane strain compressed samples as a function of the compression ratio; the trend is similar to the density behavior shown in Figure 3. Both the density and the heat of melting behavior indicate that the crystalline phase of nylon 6 samples undergoes extensive changes during the course of compression in a channel die. In Figure 5 the peak melting temperatures are plotted against sample compression ratio. The observed changes in the melting temperature suggest that the initial compression causes some further crystallization of the samples. The decrease of T_m, above a compression ratio of 1.9, suggests a partial destruction of crystals due to extensive plastic deformation. The second increase of the melting temperature above compression ratios of 2.6 indicates an increase in crystallinity of the plastically deformed material, where apparently the disrupted crystallites in the initial spherulites are being reconstituted into the final morphology of the macroscopic quasi-crystal texture.

The fractions of both crystallographic phases, α and γ, for several samples of nylon 6 taken to increasing compression ratios were obtained by deconvolution of the X-ray diffraction data and are given in Table I. (The details of

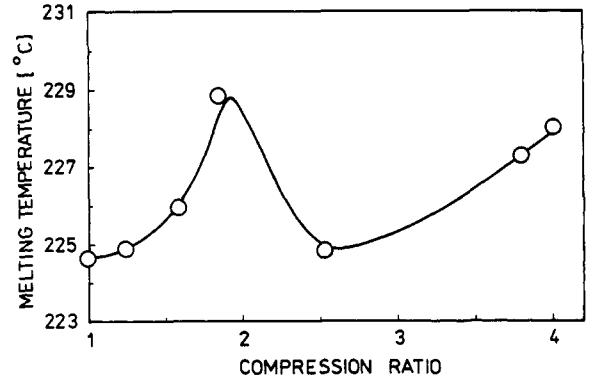

Figure 5. Melting temperature of nylon 6 samples subjected to compression in a channel die.

Table I
Degrees of Crystallinity and Weight Fraction of the α-, γ-, and Amorphous-Phase Components in Compressed Samples of Nylon 6

compression ratio	fractn α form (200) + (002) + (0 14 0)	fractn γ form (020) + (200) + (0 14 0)	fractn amorphous phase	calcd density	measd density
1.0	0.443	0.0	0.557	1.1460	1.1453
1.83	0.530	0.015	0.455	1.1597	1.1505
2.53	0.372	0.048	0.580	1.1370	1.1440
4.0	0.483	0.039	0.478	1.1550	1.1510

the computation are given in Appendix I.) The virgin, uncompressed sample contains a fraction of 0.44 of α-form crystallites and no γ form. At compression ratio of 1.84 the sample contains a fraction 0.53 of α form, and a small fraction of γ form is also found to appear. As the compression ratio increases to 2.53, the fraction of α nylon 6 drastically decreases and more γ form is produced. Further compression results in a renewed increase of the fraction of α form and a small decrease of the γ form.

Polarized light micrographs of thin sections of deformed samples are presented in Figure 6a–d. The undeformed sample shown in Figure 6a exhibits a well-developed spherulitic structure. For compressed samples in sections cut along a plane transverse to the free direction, the maltese crosses characteristic of the spherulitic radial ordering can be readily identified even at a compression ratio of 4.0, as can be seen in Figure 6b–f. The dimension of spherulitic ordering along the transverse direction does not change markedly as the compression ratio increases, while the dimension along the compression direction decreases with compression. In sections parallel to the free direction, shown in Figure 6g,h, it is seen that the spherulites become elongated along the free direction and compressed along the compression direction, as the compression ratio increases. However, at compression ratios above 1.6, as shown in Figure 6i–k, no clear spherulitic arrangement can be distinguished. Instead shear bands at −45° and +45° with respect to the free direction appear. These are identified in Figure 6j. The highest number of shear bands occurs in the sample with a compression ratio of 2.53 shown in Figure 6j. From the number and the location of shear bands it is relatively clear that the shear bands are formed preferentially at former spherulite boundaries. Further increase of the compression does not cause any significant increase in the number of shear bands. Shear bands generated at lower compression ratios, however, become tilted toward the free direction at higher compression ratios.

Parts a–c of Figure 7 are pole figures of normals to the (200) crystallographic planes of the α form of compressed nylon 6 samples. The pole figures show clearly that the (200) plane normals become systematically oriented in

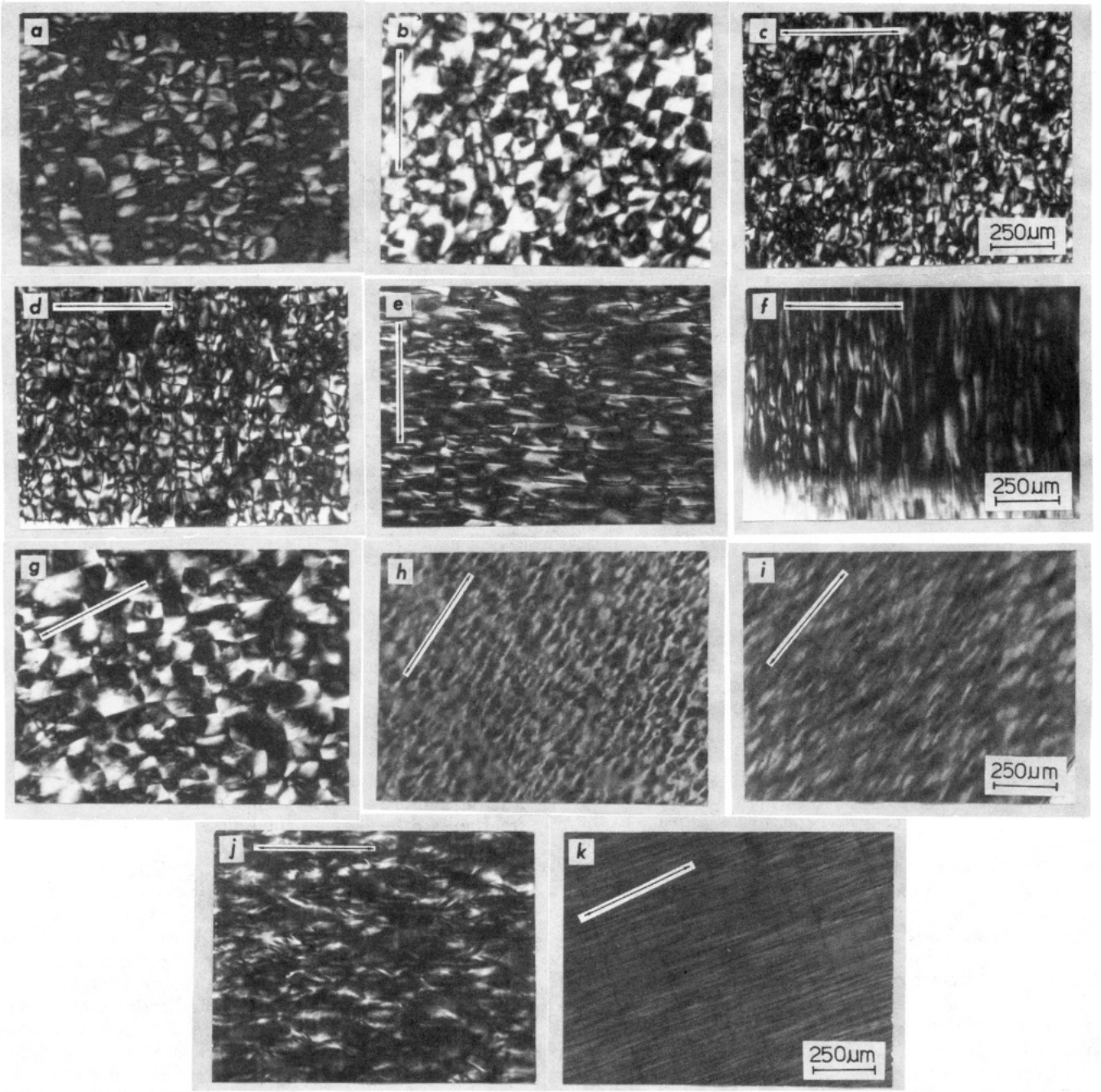

Figure 6. Polarized light micrographs of thin sections of nylon 6 samples: (a) uncompressed sample. Compressed samples sectioned perpendicularly to the free direction of a channel die and taken to compression ratios of (CD marked by arrows on figures) (b) 1.24, (c) 1.54, (d) 1.83, (e) 2.53, and (f) 4.0. Compressed samples sectioned parallel to the plane defined by the free and the compression directions. (FD marked by arrows on figures.) Compression ratios: (g) 1.24; (h) 1.54; (i) 1.83; (j) 2.53; (k) 4.0.

the transverse direction as compression increases. At the compression ratio of 4.0 (Figure 7c) the normals become perceptibly split into two groups oriented at −30° and +30° with respect to the transverse direction. The further sharpening of this bifurcation of the normals of the (200) planes in nylon 6 samples with compression ratios above 4 has been studied by Lin and Argon.[13]

Figure 8 gives pole figures of the (002) plane normals of the α form of compressed nylon 6 samples. The (002) normals become systematically oriented parallel to the compression direction as the compression ratio increases.

At compression ratios of 2.53 and above, it is possible to detect a distinct reflection from the (0 14 0) crystallographic plane of the α form of nylon 6 at a 2θ angle of around 77°. The pole figures for normals to (0 14 0) planes are shown in Figure 9. Normals to (0 14 0) planes are nearly parallel to the nylon 6 chains in α crystals. Therefore, the pole figures presented in Figure 9 are in fact pole figures of orientation of the macromolecules, and these become oriented along the flow direction as the compression ratio increases. At a compression ratio of 4.0, the orientation of macromolecules in α crystals is almost perfectly aligned with the flow direction.

Examination of the (002) peak width reveals considerable initial broadening with compression, from an average value of 0.016 at a compression ratio 1.84 to 0.020 at 2.53. For the compression ratio of 4.0, the average (002) peak width decreases to 0.014. Broadening of the peak width indicates a decrease in the α-crystal dimensions along normals to (002) planes, while the narrowing of that peak at a compression ratio of 4.0 means that the characteristic dimension of α crystals has increased in that direction. The peak width of the (200) reflection for α crystals does not undergo significant changes and remains at an average

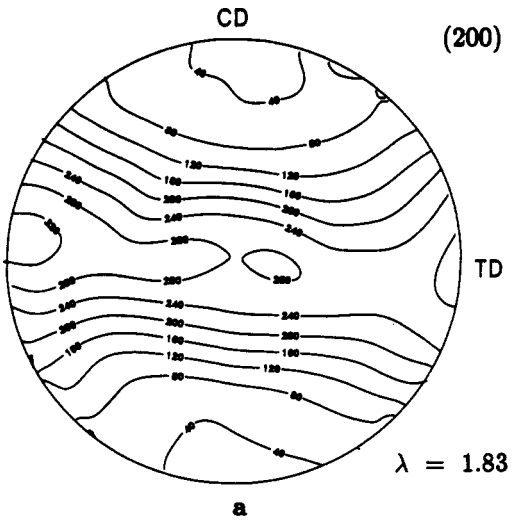

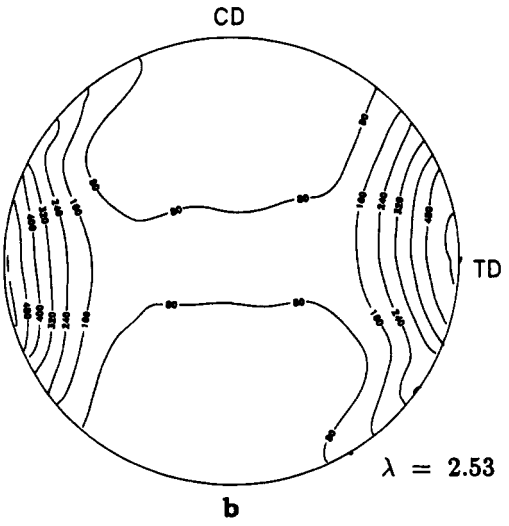

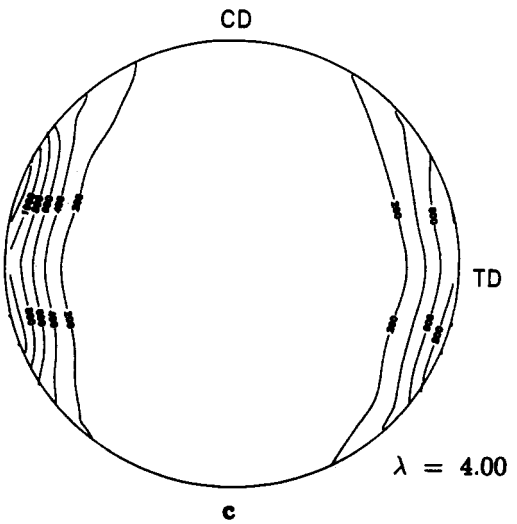

Figure 7. Pole figures of normals to (200) planes of α crystals of nylon 6 samples at compression ratios of (a) 1.83, (b) 2.53 and (c) 4.0.

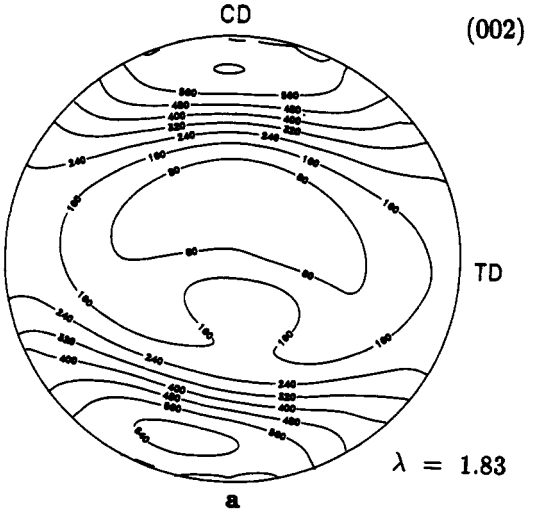

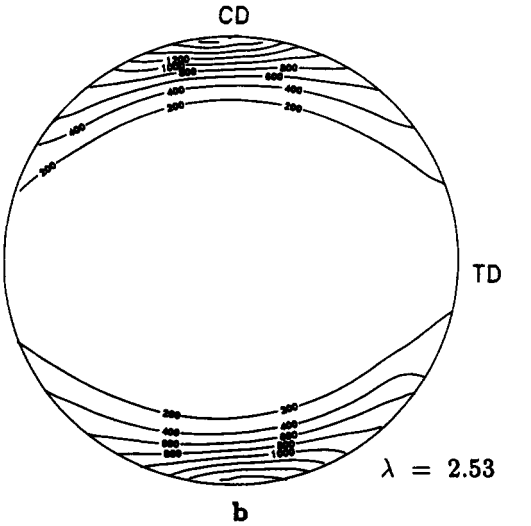

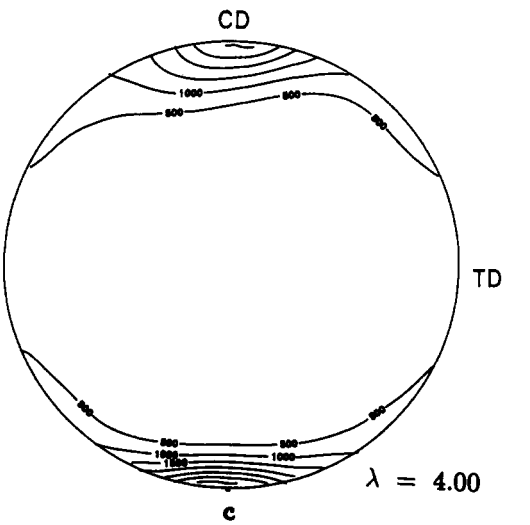

Figure 8. Pole figures of normals to (002) planes of α crystals of nylon 6 samples at compression ratios of (a) 1.83, (b) 2.53 and (c) 4.0.

value of 0.013 for all compression ratios. The pole figures of normals to (200), (002), and (0 14 0) planes of α crystals in the sample compressed to the highest ratio are shown in Figures 7c, 8c, and 9c. These pole figures suggest that the alignment of α crystals resembles a twinned monocrystal with crystallographic planes containing hydrogen bonds, the (002) planes, becoming perpendicular to the compression direction, with the macromolecular chains aligned along the flow direction. The apparent twinning symmetry plane is the (002) plane. The coherency length of these domains having an apparent twining relationship to each other has not yet been determined.

Beginning with the sample compressed to the ratio of 1.84, a fraction of γ crystals can be detected by X-ray

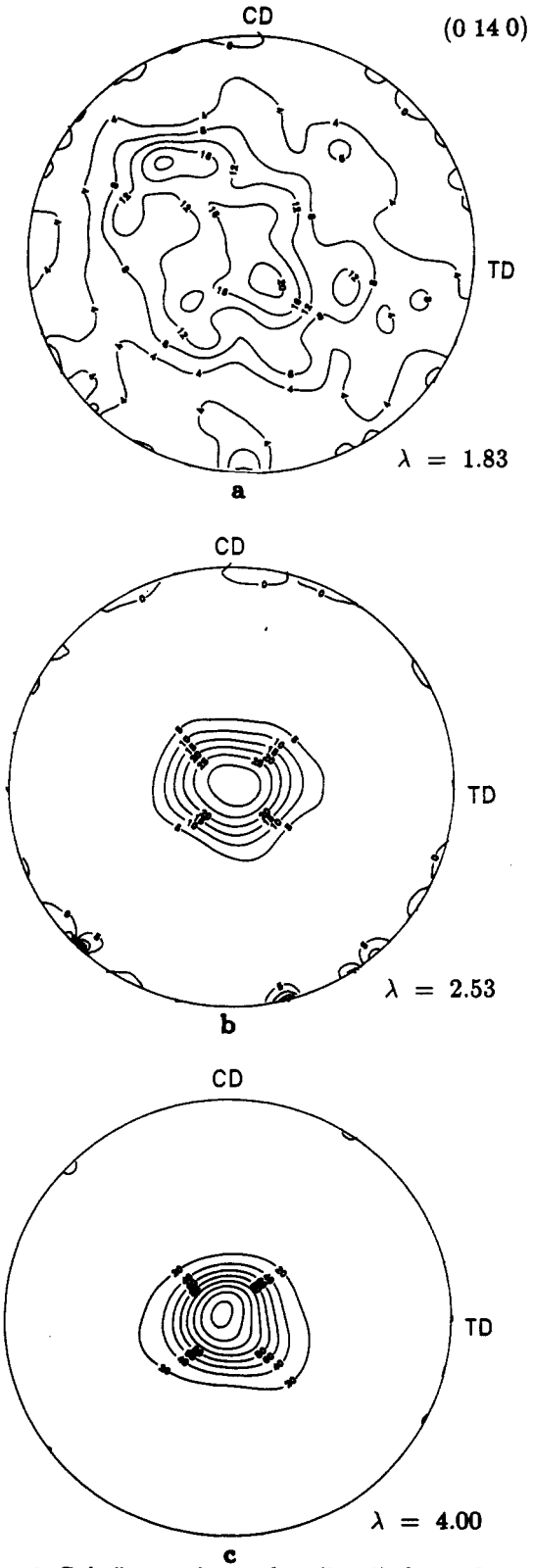

Figure 9. Pole figures of normals to (0 14 0) planes of α crystals of nylon 6 samples at compression ratios of (a) 1.83, (b) 2.53, and (c) 4.0.

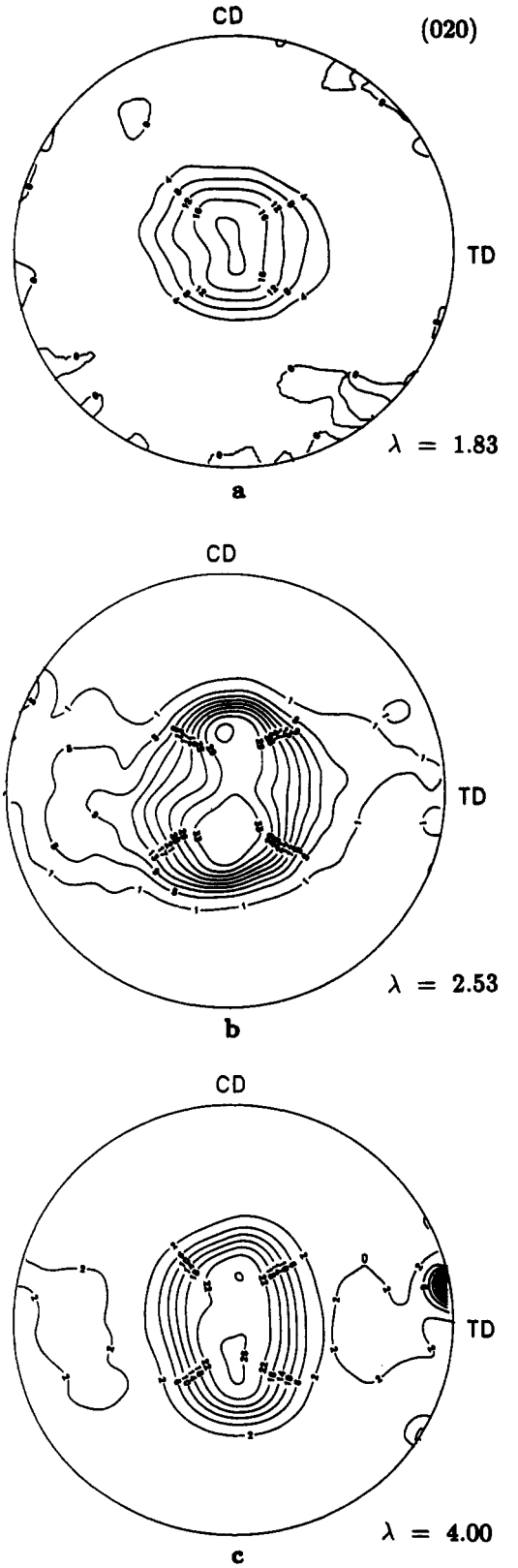

Figure 10. Pole figures of normals to (020) planes of γ crystals of nylon 6 samples at compression ratios of (a) 1.83, (b) 2.53, and (c) 4.0.

diffraction via the reflection at $2\theta = 11°$, which results from the (020) planes of the γ phase. This is shown in Figure 10. There are two preferred orientations of the nylon 6 chains in the γ crystals; they reside in a plane formed by the flow and compression directions but are inclined up and down at acute angles with respect to the flow direction. We note that chain directions in the γ crystals are very similar to the directions of the shear bands observed in the light micrographs shown in Figure 6g–h.

Pole figures of normals to the (0 14 0) planes of the γ phase are presented in parts a and b of Figure 11 for samples compressed to the ratios 2.53 and 4.0. The (0 14 0) γ phase reflection at $2\theta \simeq 81°$ was deconvoluted from the (0 14 0) reflection to the α phase, which is at 2θ around 77°. Figure 11b reinforces the observation noted above

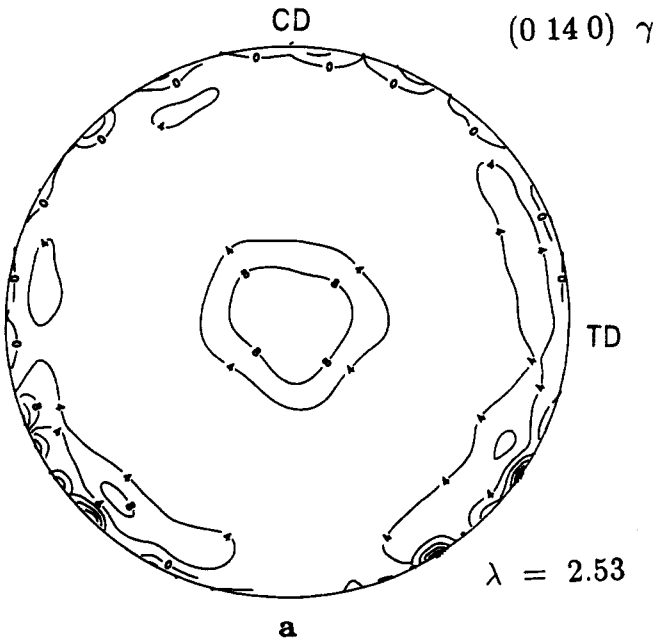

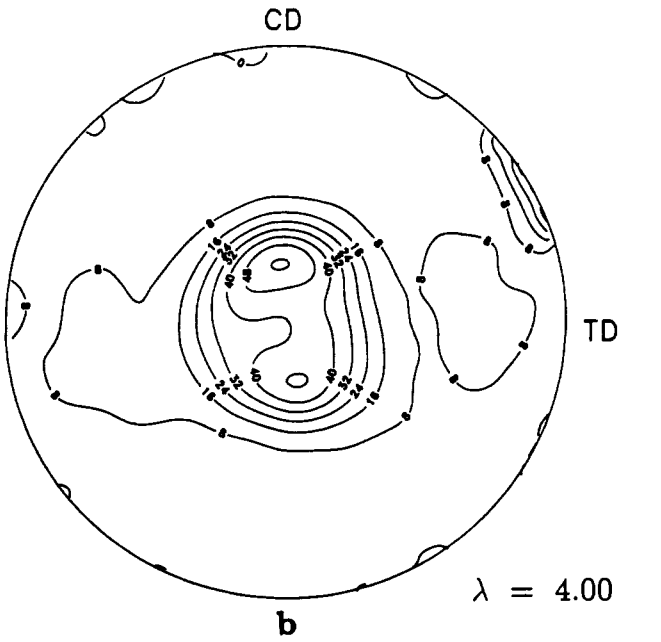

Figure 11. Pole figures of normals to (0 14 0) planes of γ crystals of nylon 6 samples at compression ratios of (a) 2.53 and (b) 4.0.

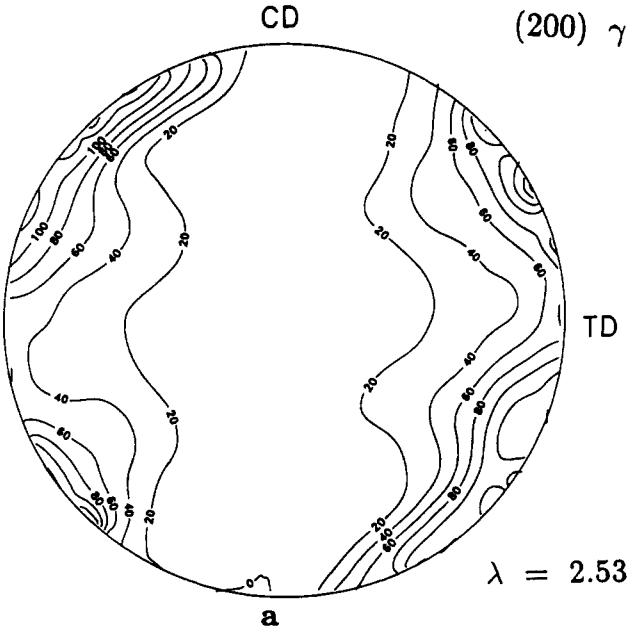

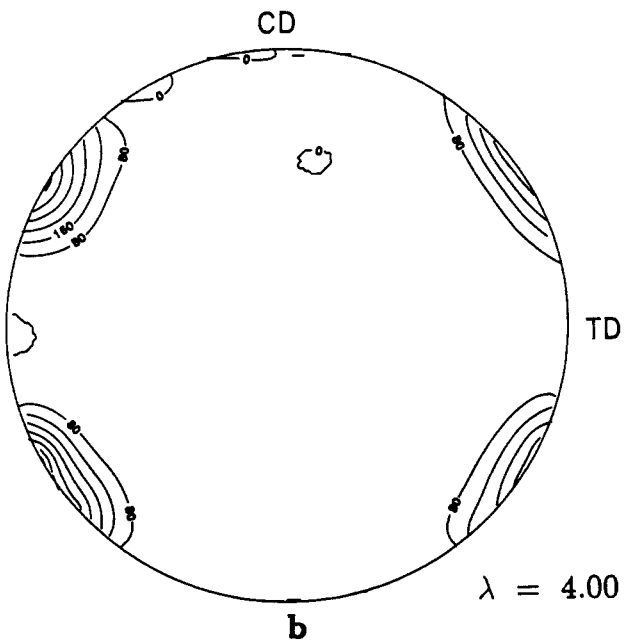

Figure 12. Pole figures of normals to (200) planes of γ crystals of nylon 6 samples at compression ratios of (a) 2.53 and (b) 4.0.

based on the (020) γ-phase pole figures, namely, that the nylon 6 chains of the γ phase reside in a plane defined by the compression and flow directions and at an angle inclined relative to the flow direction.

The other crystallographic plane of γ crystals that gives a distinct X-ray reflection is the (200) plane. The pole figures for normals to those planes for the sample compressed to the ratio of 2.53 and 4.0 are depicted in parts a and b of Figure 12. The orientations of normals to the (200) planes are concentrated in −60° and +60° fans of a pole figure with respect to the compression direction, which means that the (002) crystallographic planes of γ crystals are mostly perpendicular to the plane formed by the free and the compression directions. There is a slight tilting of the (002) planes of the γ crystals with respect to the free direction as indicated by the pole figures for normals to the (020) and (0 14 0) planes.

IV. Discussion

The array of results presented above leads to some understanding of the mechanisms of plastic deformation during plane strain (channel die) compression of nylon 6. Three important interrelated facts are (i) the formation (at compression ratios of 1.6 and greater) of shear bands that are tilted with respect to the flow direction, (ii) the first appearance of γ crystals near the same compression ratio of 1.6, and (iii) the alignment of the nylon 6 chains in γ crystals along these same shear planes. The most plausible explanation for these observations is that internal shear fields produce high orientation of fragments of macromolecular chains along shear planes. The oriented, nearly parallel fragments of macromolecules crystallize into γ crystals, thereby preserving the orientation of those fragments in the final compressed specimen.

The X-ray data on crystallinity, along with the density and heat of melting results, indicate a significant deformation-induced deterioration of α crystals during compression, beginning at a compression ratio of 1.6. The (002) peak width broadening above a compression ratio of 1.6 associated with no significant changes in the (200) peak width strongly supports the mechanism of chain slip along crystallographic planes containing hydrogen bonds, i.e., the (002) planes in α nylon 6. The chain slip mechanism in α crystals causes the observed significant decrease of the degree of crystallinity of the samples from 53 to 37 wt %. It follows then that chain slip does not by itself produce γ crystals. Slip along planes of hydrogen bonds in α crystals causes rotation of fragments of lamellae that tend to assume the orientation of (002) planes perpendicular to the compression direction in a channel die. Further compression of the samples results in an increase of a total α crystallinity and in an increase of α-crystal dimensions along normals to (002) planes. This latter effect is probably caused by a deformation-induced crystallization of macromolecular chains, straightened due to chain slip, under elevated pressure and at 150 °C, at which the compression tests were carried out.

These conclusions are supported by pole figures of intensities of the amorphous halo for compressed samples shown in Figure 13. The amorphous halo at 2θ in the range 17–23° contains largely intermolecular information (see, e.g., refs 17 and 18). For interpretation of that information knowledge of the packing of neighboring molecules is required. For the amorphous phase of nylon 6 a two-dimensional pseudohexagonal close packing is often assumed.[19] It follows then that the amorphous halo at 2θ in the range 17–23° is composed of (100) reflections. Since pole figures are maps of statistical distribution of normals to a given (*hkl*) plane, the analysis of pole figures presented in Figure 13 shows that most of the fragments of macromolecular chains in the amorphous regions of compressed nylon 6 are aligned in a plane formed by the compression direction and the free direction. Those fragments of macromolecules are inclined in that plane at an acute angle with respect to the compression direction.

Acknowledgment. This research has been supported in part by the DARPA/ONR URI program on simulation of polymer properties under Contract N00014-86-K-0768 and in part by CPBP 01.14 through the Polish Academy of Sciences. We are grateful to Mr. L. Lin for help in the plane strain compression experiments.

Appendix. Determination of Changing Fractions of Different Components of Material in Compressed Samples

The degree of crystallinity is best determined on the basis of analysis of X-ray diffraction results. In the present case such determination is estimated to have a maximum error that is less than 0.005.

The degree of crystallinity of oriented samples was obtained by integration of total intensities under rectified and deconvoluted diffraction peaks for certain crystallographic forms and for the amorphous halo over all positions (1386 positions in the present measurements) of the sample for 5° increments of the Euler angles α from 0 to 90° and β from 0 to 360° and scaled to the integrated total intensity under all diffraction peaks, with the amorphous halo background being subtracted. Thus, such degrees of crystallinity represent a weight fraction of different crystal forms in a sample. The density of a sample for known densities of all crystallographic forms and the amorphous

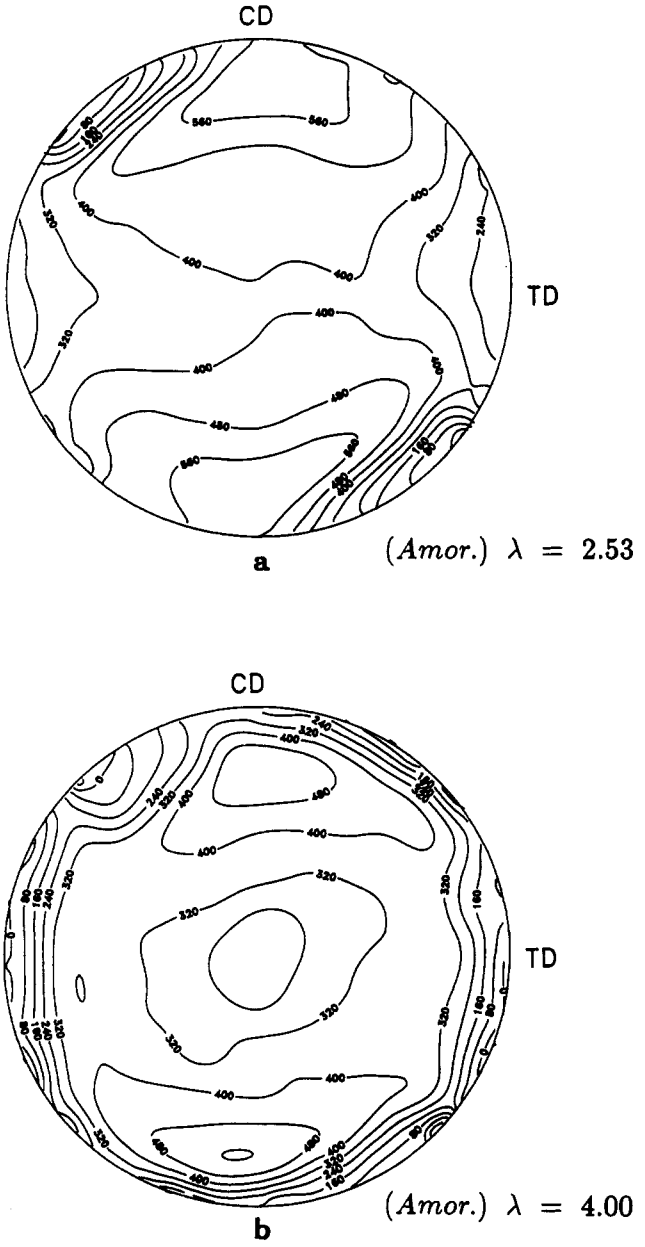

Figure 13. Pole figures of amorphous halo intensities of nylon 6 samples at compression ratios of (a) 2.53 and (b) 4.0.

phase is calculated as follows:

$$\rho = \frac{m_\alpha + m_\gamma + m_{am}}{V_\alpha + V_\gamma + V_{am}} = \frac{M}{\frac{m_\alpha}{\rho_\alpha} + \frac{m_\gamma}{\rho_\gamma} + \frac{m_{am}}{\rho_{am}}} = \frac{1}{\frac{c_\alpha}{\rho_\alpha} + \frac{c_\gamma}{\rho_\gamma} + \frac{c_{am}}{\rho_{am}}} \quad \text{(A.1)}$$

where $M = m_\alpha + m_\gamma + m_{am}$ is the total mass of the sample; m_α, m_γ, and m_{am} are the masses of the α and γ crystallographic phases and the amorphous phase, respectively; ρ_α, ρ_γ, and ρ_{am} are their densities; and c_α, c_γ, and c_{am} are their weight fractions. Such a procedure should be quite accurate for melt-crystallized samples, where the values ρ_α, ρ_γ, and ρ_{am} are precisely known. However, in plastically deformed samples all crystallographic phases are defective and stressed while the amorphous phase is nonuniformly oriented. Their densities differ markedly from those for virgin samples; defective and stressed crystals have lower density, while the oriented amorphous phase is more tightly packed and has higher density. The crystallinities and calculated and measured densities of component phases for channel die compressed nylon 6 samples are given in

Table I. These calculated densities were based on ρ_α = 1.23g/cm^3, ρ_γ = 1.17g/cm^3, and ρ_{am} = 1.08g/cm^3.

References and Notes

(1) Ode, T.; Kawai, H. *J. Polym. Sci.* **1965**, *A3*, 1943. O'Leary, K. J.; Geil, P. H. *J. Macromol. Sci.* **1962**, *B2*, 261.
(2) Zaukelies, D. A. *J. Appl. Phys.* **1962**, *33*, 2797.
(3) Bessel, T. J.; Hull, D.; Shortall, J. B. *J. Mater. Sci.* **1975**, *10*, 1127.
(4) Crist, B.; Peterlin, A. *Makromol. Chem.* **1973**, *171*, 211.
(5) Ziabicki, A. *Kolloid Z.* **1960**, *167*, 132.
(6) Lewis, E. L. V.; Ward, I. M. *J. Macromol. Sci. Phys.* **1980**, *B18*, 1; **1981**, *B18*, 75.
(7) Shaper, A.; Hirte, R., Ruscher, C.; Hillebrand, R.; Walante, E. *Colloid Polym. Sci.* **1986**, *264*, 649. Shaper, A.; Hirte, R.; Rusher, C. *Colloid Polym. Sci.* **1986**, *264*. 668.
(8) Galeski, A.; Argon, A. S.; Cohen, R. E. *Macromolecules* **1988**, *21*, 2761.
(9) Peterlin, A. *Colloid Polym. Sci.* **1975**, *253*, 809.
(10) Peterlin, A. In *Polymeric Materials*; Baer, E., Ed.; American Society for Metals: Metals Park, OH, 1975; p 175.
(11) Galeski, A.; Argon, A. S.; Cohen, R. E. *Macromol. Chem.* **1987**, *188*, 1195.
(12) Galeski, A.; Argon, A. S.; Cohen, R. E. *Macromolecules*, preceding paper in this issue.
(13) Lin, L.; Argon, A. S., unpublished results.
(14) Gray, R. W.; Young, R. J. *J. Mater. Sci.* **1974**, *9*, 521.
(15) Cullity, B. D. *Elements of X-ray Diffraction*; Addison-Wesley Publishing Co.: Reading, MA, 1978; pp 107–143, 303–316.
(16) Reference 15, pp 281–292, 447–477.
(17) Windle, A. H. In *Developments in Oriented Polymers*; Ward, I. M. Ed.; Elsevier: London, 1986; Vol. 1, pp 1–46.
(18) Owen, A. J. In *Developments in Oriented Polymers*; Ward, I. M., Ed.; Elsevier: London, 1987; Vol. 2, pp 237–268.
(19) Gurato, G.; Fichera, A.; Grandi, F. Z.; Zanetti, R.; Canal, P. *Macromol. Chem.* **1979**, *175*, 953.